Effect of cell shape on nonlinear electrophoresis migration

Viswateja Kasarabada,† Olivia D. Ernst,† Alaleh Vaghef-Koodehi,† and Blanca H. Lapizco-Encinas†,* † Microscale Bioseparations Laboratory and Biomedical Engineering Department, Rochester Institute of Technology, 160 Lomb Memorial Drive, Rochester, New York, 14623, United States. *Email: bhlbme@rit.edu

Abstract

This study contributes to the renewed interest in the study of nonlinear electrophoresis of colloidal particles. In this work the influence of cell shape on electrophoretic migration under the nonlinear regimes of moderate and strong field regimes was assessed. Four types of bacterial and yeast cells (one spherical, three non-spherical) were studied and their electrophoretic mobilities for the moderate and strong electric field magnitude regimes were estimated experimentally. The parameter of sphericity was employed to assess the effect cell shape on the nonlinear electrophoresis migration velocity and corresponding mobility under the two electric field magnitude regimes studied. As particle migration under nonlinear electrophoresis depends on particle size and shape, the results in terms of mobilities of nonlinear electrophoresis were presented as function of cell hydrodynamic diameter and sphericity. The results indicated that the magnitude of the mobilities of nonlinear electrophoresis for cells increase with increasing cell size and increase with increasing deviations from spherical shape, which is indicated by lower sphericity values. The results presented here are the very first assessment of the two types of mobilities of nonlinear electrophoresis of cells as a function of size and shape.

Keywords:

- 32 Cells
- 33 Electrophoresis
- 34 Microfluidics
- 35 Microparticles
- 36 Nonlinear Electrophoresis

1. Introduction

There is currently a renewed interest in the study of nonlinear electrophoresis and its application in microfluidic devices, in particular, for the separation and enrichment of particles of interest, including microorganisms. Several publications by Khair and Righetti et al.[1–3] have underscored that last century was marked by the major advances on linear electrophoresis, establishing it as a robust and reliable laboratory technique. As explained by Vesterberg [4], it took decades for the full acceptance of electrophoretic techniques and the development of its full analytical potential [5]. The 21st century has witnessed major developments in nonlinear electrophoresis [1], whose fundamentals were first unveiled by Dukhin decades ago [6,7]. However, the lack of experimental measurements delayed the expansion of nonlinear electrophoresis research [8].

The fundamentals established by Dukhin and collaborators [6,7] in the early 1990s have been further developed by the contributions of several groups, including Mishchuk and Barinova [8], Schnitzer and Yariv [9–11], and Shilov [12], among others. These groups have developed important analytical expressions describing the nonlinear electrophoretic migration of colloidal particles. Recent experimental studies have complemented the extensive wealth of knowledge on the theory of nonlinear electrophoresis. In particular, the experimental reports by Rouhi et al. [13], Tottori et al. [14], Cardenas-Benitez et al.[15], Bentor et al. [16,17], Ernst et al. [18], and Lomeli-Martin et al. [19], have unveiled the strong effects of nonlinear electrophoresis on particle migration

in microfluidic devices. The three former reports [13–15] illustrated that nonlinear electrophoresis is capable of particle trapping and enrichment, while the four later reports [16–19] characterized the mobility of nonlinear electrophoresis as a function of particle properties.

In this work, the effect of cell shape on the magnitude of nonlinear electrophoresis was analyzed experimentally for bacteria and yeast cells of varying sizes. Nonlinear electrophoresis, classified as a second-kind effect, depends on the bulk charge of the particle, thus, particle characteristics such as size and shape influence the magnitude of the nonlinear electrophoretic mobility [1,4,6]. In contrast, particle size and shape do not affect the mobility of linear electrophoresis [20,21]. Another distinction between linear and nonlinear electrophoresis is that the mobility of linear electrophoresis is independent of the electric field magnitude, while this is not the case for nonlinear electrophoresis. Bentor and Xuan [17] recently studied the migration on non-spherical (pear and peanut shapes) particles, in particular they studied the effects of particle orientation, particle shape and buffer concentration on particle electrophoretic velocity and its corresponding mobility under the nonlinear regime. To account for particle shape they employed the parameter of particle slenderness. The present work, is a continuation of two previous studies [18,19] dedicated to characterizing the mobilities of nonlinear electrophoresis under two distinct electric field magnitude dependencies (E^3 and $E^{3/2}$). Four distinct strains of cells (three bacteria and one yeast) with prolate, rod and spherical shapes were characterized with particle tracking velocimetry (PTV). All cells used in this study had a negative surface charge as illustrated by their zeta potentials (ζ_P) values. The parameter of sphericity was employed to assess the effect of cell shape on the nonlinear electrophoretic migration velocity and corresponding mobility under the E^3 and $E^{3/2}$ electric field magnitude dependencies. The shape parameter of sphericity was selected after a careful evaluation of four distinct shape parameters. As particle migration under nonlinear electrophoresis depends on both particle size and shape, the results in terms of mobilities of nonlinear electrophoresis were presented as function of cell hydrodynamic diameter and sphericity. The results, which agreed with theoretical studies [1,22] and previous experimental studies carried out with polystyrene particles [17– 19], showed that the magnitude of the mobility for nonlinear electrophoresis under the moderate (\mathbf{E}^3) and strong regimes $(E^{3/2})$ increase with increasing cell size and increase with increasing deviations from spherical shape which are indicated by decreasing sphericity values. The present study contributes to the ongoing growth of the field of nonlinear electrophoresis. The findings from this work are the first report on the effect of cell shape on nonlinear electrophoretic migration and have the potential to be utilized in the design of electrokinetic (EK) systems for the separation of microorganisms.

2. Theory

54

55

56

57

58

59

60

61

62

63

64

65

66

67

68

69

70

71

72

73

74

75

76

77

78

79

80

81

82 83

84

85

86

A brief summary of the theory is included here, as there are several recent publications listing this information [13–19]. The system considered here is a rectangular microchannel with a constant cross section,

which is shown in **Figure 1** stimulated with direct current (DC) electric potentials. Electrokinetic phenomena are classified on their dependence with the electric field magnitude as linear and nonlinear. The former are also called first-kind phenomena and the latter are called second-kind phenomena. The linear EK phenomena present in this system are electroosmosis (EO) and linear electrophoresis (EP_L), with the following velocity expressions:

91
$$\mathbf{v}_{EO} = \mu_{E0}\mathbf{E} = -\frac{\varepsilon_m \zeta_W}{n}\mathbf{E}$$
 (1)

92
$$\mathbf{v}_{EP,L} = \mu_{EP,L} \mathbf{E} = \frac{\varepsilon_m \zeta_P}{\eta} \mathbf{E}$$
 (weak field regime) (2)

where v is represents velocity, μ are the mobilities of EO and EP_L, ε_m and η refer to the permittivity and 93 viscosity of the suspending medium, respectively; ζ denotes the zeta potential of the channel wall or the 94 particle, and the electric field magnitude is illustrated by E. Nonlinear electrophoresis (EP_{NI}) is the only 95 nonlinear EK effect considered in the system employed illustrated in Figure 1, which can become a dominant 96 effect on particle electromigration at high electric fields. To identify the appropriate expression to describe 97 particle migration under nonlinear electrophoresis, is necessary to rely on three dimensionless quantities: the 98 dimensionless applied field magnitude (β), the Peclet (Pe) and Dukhin (Du) numbers, which are described as 99 follows: 100

$$\beta = \frac{Ea}{\omega} \tag{3}$$

$$102 Pe = \frac{a|v_{EP}|}{D} (4)$$

$$Du = \frac{K^{\sigma}}{K_m a} \tag{5}$$

where E is the magnitude of electric field, a is the particle radius, φ is the thermal voltage (~25 mV), v_{EP} is the magnitude of the electrophoretic velocity (linear and nonlinear contributions), D is the diffusion coefficient, K^{σ} and K^{m} are the surface and bulk conductivity of the medium, respectively. There two analytical expressions for the velocity of EP_{NL}, which are the limiting cases of low and high Pe numbers, described as follows [10,13]:

108
$$\mathbf{v}_{EP,NL}^{(3)} = \mu_{EP,NL}^{(3)} \mathbf{E}^3$$
 for $\beta \le 1$, $Pe << 1$ and arbitrary Du (moderate field regime) (6)

109
$$\mathbf{v}_{EP,NL}^{(3/2)} = \mu_{EP,NL}^{(3/2)} \mathbf{E}^{3/2}$$
 for $\beta > 1$, $Pe >> 1$ and $Du << 1$ (strong field regime) (7)

where $\mu_{EP,NL}$ is the mobility of the EP_{NL} velocity, which depends on the electric field magnitude. An important contrast between EP_L and EP_{NL}, is that the mobility of EP_L is independent of the electric field magnitude [1,13].

112 Considering all three EK effects, the overall particle velocity in the channel in **Figure 1a**, becomes:

$$\mathbf{v}_P = \mathbf{v}_{EP,L} + \mathbf{v}_{EO} + \mathbf{v}_{EP,NL} = \mu_{EP,L}\mathbf{E} + \mu_{EO,L}\mathbf{E} + \mu_{EP,NL}^{(n)}\mathbf{E}^n$$
(8)

where the dependency with the electric field magnitude of the EP_{NL} velocity is represented by n, which can be either \mathbf{E}^3 or $\mathbf{E}^{3/2}$. **Tables S3-S5** in the supplementary material list the detailed conditions for the three distinct regimes, the linear regime (\mathbf{E}^1), and the nonlinear regimes (\mathbf{E}^3 and $\mathbf{E}^{3/2}$), respectively. The deviation from spherical shape for each cell type was assessed in terms of the parameter sphericity (ψ) [23], defined in Eqn. (9), where V_P is the volume of the particle and A_P is the surface area of the particle, sphericity varies from 0 to 1, where 1 means a perfect sphere.

120
$$\psi = \frac{\pi^{\frac{1}{3}} (6V_P)^{\frac{2}{3}}}{A_P}$$
 (9)

Calculations of four distinct shape parameters for each cell type were carried out to select the best parameter to be used in this study. The discussion on the appropriate shape parameter selected is included in **Section 4.1**. A Table listing the values of the four distinct shape parameters calculated for each particle and cells is included in the supplementary as **Table S1**.

3. Materials and Methods

3.1 Microdevices

121

122

123

124125

126

127

132

138139

140

141

142

143

144

145

146

147

- Rectangular microchannels with a constant cross section were fabricated from polydimethylsiloxane (PDMS,
- Dow Corning, MI, USA) employing standard cast molding techniques [18,19]. An illustration of the
- microchannel, depicting all dimensions, is included in **Figure 1**. PTV assessments were performed at the
- microchannel center.

3.2 Suspending medium

A low conductivity solution of 0.2 mM K₂HPO₄ was employed as suspending medium, with the addition of 0.05% (v/v) Tween 20 to prevent particle adhesion. This solution had a pH of 7.4 ± 0.5 and a specific conductivity of 39.2 ± 2.2 µS/cm. These conditions produced a wall zeta potential $\zeta_W = -60.1 \pm 3.7$ mV and $\mu_{EO} = 4.7 \pm 0.3 \times 10^{-8} m^2 V^{-1} s^{-1}$ in the PDMS devices as assessed with current monitoring [24]. The thickness of the electrical double layer (EDL) was estimated as 14 nm.

3.3 Bacterial and yeast cells

Four distinct types of cells (three bacteria and one yeast) were studied, and their characteristics, including their American Type Culture Collection (ATCC) numbers, are listed in **Table 2**. To enable visualization, cells were labeled with fluorescent dyes (SYTO® dyes, Thermo Fisher Scientific, Carlsbad CA). Sample suspensions of cells were prepared with concentrations between 2.9 to 6.0 x 10⁷ cells/mL as listed in **Table S2**. Cell concentrations were adjusted to allow tracking visibility.

3.4 Equipment and software.

PTV experiments were recorded with a Leica DMi8 (Wetzlar, Germany) and a Zeiss Axiovert 40 CFL (Carl Zeiss Microscopy, Thornwood, NY) inverted microscopes equipped with a color camera. Direct current potentials were applied employing a high voltage power supply (Model HVS6000D, LabSmith, Livermore, CA)

which was controlled with the software *Sequencer* provided by the manufacturer. Platinum electrodes were connected to the power supply to apply DC potentials to the microdevices.

3.5 Experimental procedure

To ensure stable EO flow, all PTV devices were conditioned before experiments by soaking the channels with the suspending medium for 8-12 hours. Prior to each experiment, channels were filled out with the suspending medium and pressure-drive flow was minimized. A sample of the selected cell suspension (1 μ L to 2 μ L) of was added to the inlet reservoir of the microchannel and followed by placement of the electrodes at both reservoirs. To perform PTV assessments, electric potentials were applied for 15 seconds while simultaneously recording images. The results from low voltage PTV experiments were used to estimate ζ_P and $\mu_{EP,L}$ values, the experiments were run between 25-150 Volts to ensure a Pe value below 1 and linear dependence on E (see Table S3). High voltage PTV experiments run between 100-3000 Volts to were used to assess electrophoretic velocities under the moderate and strong field regimes (see Tables S4-S5, respectively). All experiments were run in triplicate and analyzed using ImageJ and Tracker software to determine cell velocity.

4. Results and Discussion

4.1 Selection of the parameter to define cell shape deviations from spherical shape

A careful analysis of the appropriate parameters to describe particle shape as it deviates from the spherical shape was necessary in this study. This is perhaps an unexplored area in iEK separations, since there are not many reports that have focused on the effect of particle or cell shape on their electromigration. Recently, Bentor and Xuan [17] utilized the parameter slenderness to describe particle shape in a study that investigated the electrophoretic migration of various shaped synthetic particles. In the present study, four distinct shape parameters utilized in geology [25] were analyzed to better understand the relationship between cell shape and the electrophoretic properties of the cells assessed in this work. The four shape parameters considered were: circularity, sphericity (ψ), slenderness and ISO roundness. Of these parameters, sphericity was selected due to its three-dimensional characterization of cells as opposed to the two-dimensional parameters of circularity, slenderness and ISO roundness. The sphericity values of the cells varied depending on the overall cell shape. For example, the sphericity of prolate and rod shaped bacteria varied between 0.72-0.78. A sphericity values of 1.0 was obtained for the spherical yeast cells.

Since particle migration under EP_{NL} is affected by both particle size and shape [1], it was necessary to consider both parameters, cell size and shape, in the assessment of the mobilities of EP_{NL} . From the recent report by Bentor and Xuan [17] it was observed that the magnitudes of the mobilities of EP_{NL} increased as particle shape deviated from the spherical shape. In their study [17], they employed three types of polystyrene particles

of similar size (equivalent diameter between 4.2 to 5.0 μ m) and distinct shapes (sphere, pear and peanut), where the peanut-shaped particle was the one that deviated the most from spherical shape (slenderness = 0.58) and also the one with the highest mobility magnitudes. Thus, it can be stated that as the sphericity of a particle decreases (increasing deviation from spherical shape), the magnitude of the mobility of EP_{NL} increases. Regarding particle size, our recent work [18] demonstrated experimentally that the magnitude of the mobilities of EP_{NL} increase with increasing particle size, which had been theorized in the fields of colloid science by Dukhin [6] and Khair [1], among others. This increase in magnitude of the mobility values is the result of a larger conductive-diffuse layer in the electrical double layer (EDL) of the particle, which in turn increases the polarization charge in the EDL. Considering the distinct and opposite effects that particle size and particle shape have on the magnitudes of the mobilities of EP_{NL} , it was decided to plot the magnitudes of the mobilities of EP_{NL} as functions of the cell hydrodynamic diameter divided by cell sphericity, as this considers both the effects of cell size and shape. These results are included in **Figure 2**.

4. 2 Effect of cell size and shape on nonlinear electrophoretic migration of bacterial and yeast cells

As it was expected from the recent study by Bentor and Xuan [17], the effects of EP_{NL} were more evident in cells with lower sphericity values, *i.e.*, cell shapes that are deviate more from spherical shape. **Figure 2** contains the results of the assessment of the migration velocity of the four distinct cell types under the influence of EP_{NL} effects. **Figures 2a-2b** illustrate the overall particle velocity (Eq. 8) and the particle EP velocity ($\mathbf{v}_{EP,L} + \mathbf{v}_{EP,NL}$) as a function of the electric field, respectively. From **Figure 2a**, As anticipated, all cell types cross the zero velocity line ($\mathbf{v}_P = 0$), this condition is called is called the electrokinetic equilibrium condition (\mathbf{E}_{EEC}) [15,19,26]. The \mathbf{E}_{EEC} is included in **Table 1**, which as observed in previous experimental studies, is a function of cell charge (ζ_P) and cell size, and as unveiled here, is as also function of cell shape; \mathbf{E}_{EEC} values decrease with increasing magnitude of ζ_P and cell size, and increase with decreasing values of cell sphericity.

As shown in **Figure 2b**, all cell types have an increasing magnitude of their EP velocity as the **E** increases (EP velocity is negative, thus, the absolute value was plotted in the figure). This is the anticipated behavior, as the magnitude of the electrophoretic velocity ($\mathbf{v}_{EP,L} + \mathbf{v}_{EP,NL}$) increases more rapidly as the electric field magnitude increases and the nonlinear effects appear [16,18,19].

4.3 Effect of cell size and shape on the magnitude of the mobilities of nonlinear electrophoresis under the moderate and strong regimes

Regarding the effect of cell size and shape on the magnitude of the electrophoretic mobilities of the under the moderate (\mathbf{E}^3) and strong regimes ($\mathbf{E}^{3/2}$), the same trends is observed for both, $\mu_{EP,NL}^{(3)}$ and $\mu_{EP,NL}^{(3/2)}$, the magnitude of these two negative mobilities increases as a function of the size/shape parameter (hydrodynamic

diameter/sphericity). These observations agree with the literature, as larger size cells have a larger magnitude of the mobility of EP_{NL} [1,6,18] due to a larger conductive-diffuse layer; and cells with larger deviations from spherical shape, which is indicated by lower sphericity values, also exhibit larger magnitudes in their mobilities of EP_{NL} as recently demonstrated by Bentor and Xuan [17]. The results in **Figures 3a-3b** are the very first assessment of the two types of mobilities of EP_{NL} of cells as a function of cell size and shape.

217218

219

220

221

222

223224

225

226

227

228

229

230

231

232

233

234

213

214

215

216

5. Conclusions

The present study contributes to the dynamic field of nonlinear electrophoresis of colloidal particles, several recent studies have already assessed the effect of particle size and particle charge on nonlinear electrophoretic migration. The present studies the effect of cell shape on nonlinear electrophoretic migration. To quantify the shape of the cells in this work, the parameter of sphericity was selected after a careful evaluation of four distinct shape parameters. Two distinct nonlinear electrophoresis regimes were studied, the moderate regime which has a cubic dependance with the electric field magnitude and the strong field regime which has a 3/2 dependance with the electric field magnitude. All cells were characterized electrokinetically employing PTV experiments in order to estimate the zeta potential and the electrophoretic mobilities under the two electric field magnitude regimes. As cell migration under nonlinear electrophoresis depends on cell size and shape, the results in terms of the magnitude of the mobilities of nonlinear electrophoresis under both regimes (moderate and strong) were presented as function of cell hydrodynamic diameter and sphericity. The result indicated that the magnitude of the mobilities of nonlinear electrophoresis increase with increasing cell size and increasing deviation from spherical shape. These results are in agreement with recent theoretical and experimental studies obtained with polystyrene particles. These findings are the first study on the effect of cell shape on nonlinear electrophoretic migration. The new knowledge produced in this work can be used to design electrokinetic-based separation of microorganisms by exploiting differences in cell shape.

235236

237

239

Declaration of Competing Interest

The authors declare no competing financial interest.

CRediT authorship contribution statement

- VK: Experimentation, Data Analysis, Writing Original Draft Review & Editing. ODE: Experimentation, Data
- Analysis, Writing Original Draft Review & Editing. AVK: Experimentation, Data Analysis, Review &
- 242 Editing. **BHLE**: Conceptualization, Methodology, Project administration, Supervision, Writing Original Draft –
- 243 Review & Editing.

Data availability

244

246

The data that support the findings of this study will be made available on request.

Acknowledgments

- This material is based upon work supported by the National Science Foundation under Awards No. 2127592
- and No. 2133207. The authors would like to thank Gabriela Martinez for assistance with experiments and Sam
- Lee for assistance in image production.

250 Supplementary material

- Supplementary material associated with this article can be found in the online version, at XXXX. This
- supplementary material file contains a table listing the four distinct shape parameters analyzed in this study, the
- cell concentration information, and the conditions employed to characterize the weak, moderate and strong field
- regimes of nonlinear electrophoresis.

255 ORCID

257

258

256 Blanca H. Lapizco-Encinas: 0000-0001-6283-8210

References

- 259 [1] A.S. Khair, Nonlinear electrophoresis of colloidal particles, Curr. Opin. Colloid Interface Sci. 59 (2022) 101587. https://doi.org/10.1016/j.cocis.2022.101587.
- P.G. Righetti, G. Candiano, Recent advances in electrophoretic techniques for the characterization of protein biomolecules: A poker of aces, J. Chromatogr. A. 1218 (2011) 8727–8737.
- https://doi.org/10.1016/j.chroma.2011.04.011.
- 264 [3] P.G. Righetti, 50, 100, 1000 Years: Happy Anniversary Electrophoresis!, Electrophoresis. 40 (2019) 11–15. https://doi.org/10.1002/elps.201800447.
- O. Vesterberg, A short history of electrophoretic methods, Electrophoresis. 14 (1993) 1243–1249. https://doi.org/10.1002/elps.11501401188.
- B.H. Lapizco-Encinas, Y.V. Zhang, P.P. Gqamana, J. Lavicka, F. Foret, Capillary electrophoresis as a sample separation step to mass spectrometry analysis: A primer, TrAC Trends Anal. Chem. 164 (2023) 117093. https://doi.org/10.1016/j.trac.2023.117093.
- 271 [6] S.S. Dukhin, Electrokinetic phenomena of the second kind and their applications, Adv. Colloid Interface 272 Sci. 35 (1991) 173–196. https://doi.org/10.1016/0001-8686(91)80022-C.
- 273 [7] S.S. Dukhin, Electrophoresis at large peclet numbers, Adv. Colloid Interface Sci. 36 (1991) 219–248. 274 https://doi.org/10.1016/0001-8686(91)80034-H.
- N.A. Mishchuk, N.O. Barinova, Theoretical and experimental study of nonlinear electrophoresis, Colloid

- J. 73 (2011) 88–96. https://doi.org/10.1134/S1061933X11010133.
- O. Schnitzer, E. Yariv, Macroscale description of electrokinetic flows at large zeta potentials: Nonlinear surface conduction, Phys. Rev. E. 86 (2012) 021503. https://doi.org/10.1103/PhysRevE.86.021503.
- [10] O. Schnitzer, E. Yariv, Nonlinear electrophoresis at arbitrary field strengths: Small-Dukhin-number analysis, Phys. Fluids. 26 (2014) 122002. https://doi.org/10.1063/1.4902331.
- O. Schnitzer, R. Zeyde, I. Yavneh, E. Yariv, Weakly nonlinear electrophoresis of a highly charged colloidal particle, Phys. Fluids. 25 (2013) 052004. https://doi.org/10.1063/1.4804672.
- V. Shilov, S. Barany, C. Grosse, O. Shramko, Field-induced disturbance of the double layer electroneutrality and non-linear electrophoresis, Adv. Colloid Interface Sci. 104 (2003) 159–173.

 https://doi.org/10.1016/S0001-8686(03)00040-X.
- [13] M. Rouhi Youssefi, F.J. Diez, Ultrafast electrokinetics, Electrophoresis. 37 (2016) 692–698.
 https://doi.org/10.1002/elps.201500392.
- [14] S. Tottori, K. Misiunas, U.F. Keyser, D.J. Bonthuis, Nonlinear Electrophoresis of Highly Charged
 Nonpolarizable Particles, Phys. Rev. Lett. 123 (2019) 14502.
 https://doi.org/10.1103/PhysRevLett.123.014502.
- 291 [15] B. Cardenas-Benitez, B. Jind, R.C. Gallo-Villanueva, S.O. Martinez-Chapa, B.H. Lapizco-Encinas, V.H.
 292 Perez-Gonzalez, Direct Current Electrokinetic Particle Trapping in Insulator-Based Microfluidics:
- 293 Theory and Experiments, Anal. Chem. 92 (2020) 12871–12879.
- https://doi.org/10.1021/acs.analchem.0c01303.
- J. Bentor, H. Dort, R.A. Chitrao, Y. Zhang, X. Xuan, Nonlinear electrophoresis of dielectric particles in Newtonian fluids, Electrophoresis. 44 (2023) 938–946. https://doi.org/10.1002/elps.202200213.
- J. Bentor, X. Xuan, Nonlinear electrophoresis of nonspherical particles in a rectangular microchannel, Electrophoresis. (2023). https://doi.org/10.1002/ELPS.202300188.
- O.D. Ernst, A. Vaghef-Koodehi, C. Dillis, A. Lomeli-Martin, B.H. Lapizco-Encinas, Dependence of Nonlinear Electrophoresis on Particle Size and Electrical Charge, Anal. Chem. 95 (2023) 6595–6602. https://doi.org/10.1021/acs.analchem.2c05595.
- A. Lomeli-Martin, O.D. Ernst, B. Cardenas-Benitez, R. Cobos, A.S. Khair, B.H. Lapizco-Encinas, Characterization of the Nonlinear Electrophoretic Behavior of Colloidal Particles in a Microfluidic Channel, Anal. Chem. 95 (2023) 6740–6747. https://doi.org/10.1021/acs.analchem.3c00782.
- D. Li, Chapter 9 Electrophoretic motion of particles in microchannels, in: Interface Sci. Technol., 2004: pp. 542–616. https://doi.org/10.1016/S1573-4285(04)80031-0.
- F.A. Morrison, Electrophoresis of a particle of arbitrary shape, J. Colloid Interface Sci. 34 (1970) 210–
 214. https://doi.org/10.1016/0021-9797(70)90171-2.
- 309 [22] S.S. Dukhin, Electrophoresis at large peclet numbers, Adv. Colloid Interface Sci. 36 (1991) 219–248.

310		https://doi.org/10.1016/0001-8686(91)80034-H.
311	[23]	H. Wadell, Volume, Shape, and Roundness of Rock Particles, J. Geol. 40 (1932) 443-451.
312		https://doi.org/10.1086/623964.
313	[24]	M.A. Saucedo-Espinosa, B.H. Lapizco-Encinas, Refinement of current monitoring methodology for
314		$electroosmotic \ flow \ assessment \ under \ low \ ionic \ strength \ conditions, \ Biomicrofluidics. \ 10 \ (2016) \ 033104.$
315		https://doi.org/10.1063/1.4953183.
316	[25]	Y. Kim, J. Ma, S.Y. Lim, J.Y. Song, T.S. Yun, Determination of shape parameters of sands: a deep
317		learning approach, Acta Geotech. 17 (2022) 1521–1531. https://doi.org/10.1007/s11440-022-01464-1.
318	[26]	S. Antunez-Vela, V.H. Perez-Gonzalez, A. Coll De Peña, C.J. Lentz, B.H. Lapizco-Encinas,
319		Simultaneous Determination of Linear and Nonlinear Electrophoretic Mobilities of Cells and
320		Microparticles, Anal. Chem. 92 (2020) 14885–14891. https://doi.org/10.1021/acs.analchem.0c03525.
321		
322		

TABLES

Table 1. Characteristics of the cells used in this study.

Cell ID	Dimensions (μm)	Hydrodynamic diameter (µm)	Sphericity	ζ _P (mV)	$\mu_{EP,L} \times 10^{-8}$ $(\text{m}^2\text{V}^{-1}\text{s}^{-1})$	E for $\mu_{EP,NL}^{(3)}$ estimation (V/cm)	$\mu_{EP,NL}^{(3)}$ x 10 ⁻¹⁸ (m ⁴ V ⁻³ s ⁻¹)	E for $\mu_{EP,NL}^{(3/2)}$ estimation (V/cm)	$\mu_{EP,NL}^{(3/2)} \times 10^{-11}$ $(m^{5/2}V^{-3/2}s^{-1})$	E _{EEC} (V/cm)
<i>E. coli</i> ATCC # 11775	L: 3.2±0.3 W: 1.1±0.2	1.8	0.78	-25.5±1.5	-3.9±0.3	500	-6.4±0.8	3000	-4.1±1.1	911.6
B. subtilis ATCC # 6051	L: 7.7±1.1 W: 1.8±0.3	3.3	0.72	-30.1±5.9	-2.3±0.5	250	-29.0±16.4	2000	-7.9±2.1	287.0
<i>B. cereus</i> ATCC # 14579	L: 4.8±0.5 W: 1.5±0.2	2.5	0.77	-46.1±3.1	-3.6±0.3	250	-4.3±3.4	2000	-5.2±1.6	518.6
S. cerevisiae ATCC # 9080	D: 5.8±0.5	5.8	1.00	-41.5±2.0	-3.2±0.2	100	-21.6±1.0	600	-14.0±3.1	318.4

D: diameter, L: length, W: width, , $\mu_{EP,L}$: mobility of linear electrophoretic velocity, $\mu_{EP,NL}^{(3)}$: cubic mobility of nonlinear electrophoretic velocity, $\mu_{EP,NL}^{(3/2)}$: 3/2 mobility of nonlinear electrophoretic velocity, E_{EEC} electrokinetic equilibrium condition

FIGURES

PTV interrogation region

0.88 mm

10.16 mm

Figure 1. Representation of the microchannel used for PTV assessments, including dimensions.

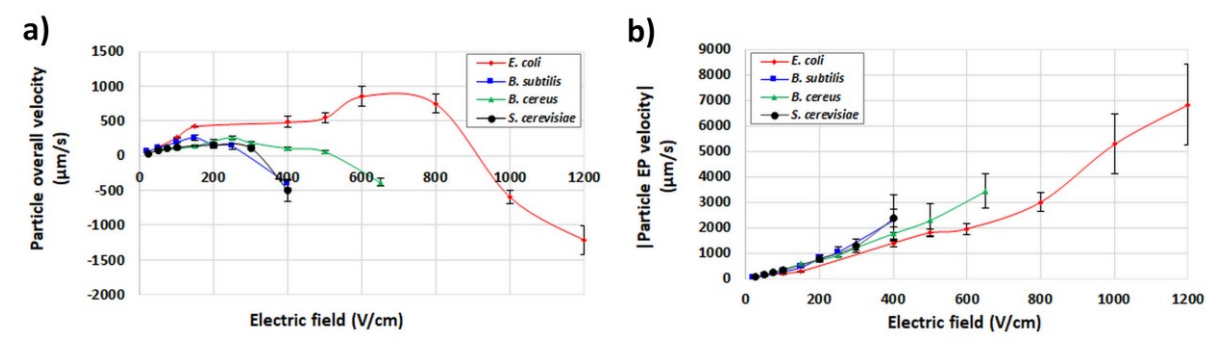


Figure 2. Plots of the (a) overall cell velocity (\mathbf{v}_P) and (b) absolute value of the cell electrophoretic velocity (linear and nonlinear contributions) as a function of the electric field. Absolute values were plotted for the electrophoretic velocities to aid visualization as these values are negative.

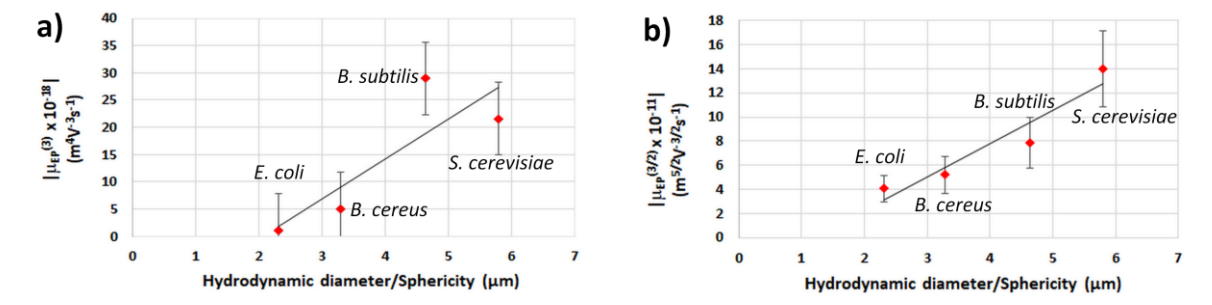


Figure 3. Plots of the absolute values of the of the magnitudes of (a) $\mu_{EP,NL}^{(3)}$ and (b) $\mu_{EP,NL}^{(3/2)}$ as a function of cell size and cell shape (hydrodynamic diameter/sphericity), respectively. Absolute values were plotted for the mobilities to aid visualization as these values are negative.